Revised MICROBIO-2023-170-RA

A tunable genetic switch for tight control of *tac* promoters in *Escherichia coli* boosts expression of synthetic injectisomes

Alejandro Asensio-Calavia[1a], Álvaro Ceballos-Munuera[1,2,b], Almudena Méndez-Pérez[1,2,c], Beatriz Álvarez[1,d] and Luis Ángel Fernández[1,e]*

(1) *Department of Microbial Biotechnology, Centro Nacional de Biotecnología, Consejo Superior de Investigaciones Científicas (CNB-CSIC), Darwin 3, Campus Cantoblanco, 28049 Madrid, Spain.*

(2) *Programa de Doctorado en Biociencias Moleculares. Universidad Autónoma de Madrid (UAM). Campus Cantoblanco, 28049 Madrid, Spain.*

a- ORCID: 0000-0001-8113-6599

b- ORCID: 0000-0002-9735-2111

c- ORCID: 0000-0001-8072-9034

d- ORCID: 0000-0002-9613-5473

e- ORCID: 0000-0001-5920-0638

*** Corresponding author:** Luis Ángel Fernández; E-mail: lafdez@cnb.csic.es; Phone: +34 91 585 4854; Fax: +34 91 585 4506;

Keywords: *E. coli*, genetic circuit, injectisome, LacI, TetR, *tac* promoter, transcriptional repressor, type III secretion system

Abstract

Biosafety of engineered bacteria as living therapeutics requires a tight regulation to control the specific delivery of protein effectors, maintaining minimum leakiness in the uninduced (OFF) state and efficient expression in the induced (ON) state. Here, we report a three repressors (3R) genetic circuit that tightly regulates the expression of multiple *tac* promoters (*Ptac*) integrated in the chromosome of *E. coli* and drives the expression of a complex type III secretion system injectisome for therapeutic protein delivery. The 3R genetic switch is based on the tetracycline repressor (TetR), the non-inducible lambda repressor cI (ind-), and a mutant *lac* repressor ($LacI^{W220F}$) with higher activity. The 3R switch was optimized with different protein translation and degradation signals that control the levels of $LacI^{W220F}$. We demonstrate the ability of an optimized switch to fully repress the strong leakiness of the *Ptac* promoters in the OFF state while triggering their efficient activation in the ON state with anhydrotetracycline (aTc), an inducer suitable for *in vivo* use. The implementation of the optimized 3R switch in the engineered Synthetic Injector *E. coli* (SIEC) strain boosts expression of injectisomes upon aTc induction, while maintaining a silent OFF state that preserves normal growth in the absence of the inducer. Since *Ptac* is a commonly used promoter, the 3R switch may have multiple applications for tight control of protein expression in *E. coli*. In addition, the modularity of the 3R switch may enable its tuning for the control of *Ptac* promoters with different inducers.

Introduction

Synthetic biology applies engineering principles on molecular systems to program living entities with defined functionalities (Brooks and Alper, 2021, Cubillos-Ruiz, et al., 2021). The implementation of functional modules in an engineered cell requires of regulatory modules to control gene expression, which often involve genetic circuits that sense external input signals and respond with defined outputs (Brophy and Voigt, 2014, Riglar and Silver, 2018). These circuits are assembled with genetic parts such as promoters, transcription factors (repressors and activators), terminators, ribosome binding sites (RBS) and protein degradation signals, which are interconnected creating systems with predictable behaviors (Voigt, 2006, Brophy and Voigt, 2014).

A promising application of synthetic biology is the development of living therapeutics, engineered cells with controlled capacities to deliver therapeutic payloads against diseases (e.g. autoimmune disorders, cancer, infections, etc.) (Piñero-Lambea, et al., 2015, Ozdemir, et al., 2018, Riglar and Silver, 2018). Given their simplicity, engineering bacterial cells for delivery of therapeutic cargoes presents unique advantages such as facilitating design and manufacturing. Interestingly, bacteria have naturally evolved molecular systems for delivery of protein payloads into host cells during infection (Costa, et al., 2015), such as the type III secretion system (T3SS) found in many Gram-negative pathogens (Galan and Wolf-Watz, 2006, Deng, et al., 2017). T3SS assembles large macromolecular protein complexes, called injectisomes, which act as nanosyringes for the active translocation of proteins into the host cell cytoplasm (Gaytan, et al., 2016, Portaliou, et al., 2016). Injectisomes comprise a multiring structure, called the needle complex, that span the inner membrane (IM), the periplasm, and the outer membrane (OM) of the bacterium, and project an extracellular needle-like hollow conduit for the passage of the secreted proteins (Butan, et al., 2019, Hu, et al., 2019). Proteins secreted by injectisomes include the translocon and effector proteins (Gaytan, et al., 2016,

Portaliou, et al., 2016). Translocon proteins insert into host plasma membrane and form a pore that is used by effectors to enter the cytoplasm of the host cell.

Injectisomes have been explored for delivery of therapeutic proteins (Blanco-Toribio, et al., 2010, Ittig, et al., 2015, Walker, et al., 2017, Bai, et al., 2018). Previous work from our laboratory reported the expression of functional injectisomes from enteropathogenic *Escherichia coli* (EPEC) in the commensal *E. coli* K-12 strain (Ruano-Gallego, et al., 2015). The resulting engineered bacterium, called Synthetic Injector *E. coli* (SIEC), contained five synthetic operons, encoding all the components needed to assemble EPEC injectisomes (Figure 1). These synthetic operons (called *eLEE1* to *eLEE4*, and *eEscD*) were controlled by the *tac* promoter (*Ptac*) (de Boer, et al., 1983). Addition of isopropyl β-D-1-thiogalactopyranoside (IPTG) inhibits the binding of the endogenous LacI repressor of *E. coli* K-12 to the *Ptac* promoters, enabling the simultaneous expression of these synthetic operons in SIEC (Ruano-Gallego, et al., 2015).

Although IPTG is effective for *in vitro* studies, this inducer has important limitations for its *in vivo* use. First, IPTG has a short half-life *in vivo* (Wyborski and Short, 1991) and can be toxic (Kosinski, et al., 1992, Dvorak, et al., 2015). Secondly, IPTG regulation suffers the intrinsic leakiness of the *lacI-Ptac* system (Wilson, et al., 2007). Leaky expression of T3SS components was observed in SIEC in the absence of IPTG, with some structural proteins reaching up to ~65% of the level found when the inducer was present (Ruano-Gallego, et al., 2015). For both biosafety and specificity of protein delivery, it is important to keep expression of injectisomes in a tight OFF state, with minimum leakiness, until the inducer is added to switch ON expression. Hence, a regulatory switch with digital OFF/ON behavior and dependent of an inducer compatible with its *in vivo* use would be advantageous for effective control of injectisomes and the development of living therapeutics.

Here, we describe the design and optimization of a tunable genetic circuit that tightly controls multiple *Ptac* promoters integrated in the chromosome of *E. coli* triggering a strong upregulation of their expression upon induction with anhydrotetracycline (aTc), an inducer suitable for *in vivo* application given its low toxicity, cell permeability and slow degradation *in vivo* (Chopra and Roberts, 2001, Berens and Hillen, 2003, Loessner, et al., 2009, Politi, et al., 2014). This molecule can be administered through different routes, including oral administration, it is effective as inducer at low concentrations, and it does not inhibit the growth of *E. coli* (Loessner, et al., 2009, Leventhal, et al., 2020). This novel genetic module uses a combination of the tetracycline repressor (TetR) (Bertram and Hillen, 2008, Bertram, et al., 2022) and of the non-inducible bacteriophage lambda repressor cI (ind-) (Sauer, et al., 1982, Gimble and Sauer, 1986) to ultimately control the expression of $LacI^{W220F}$, a mutant of LacI with higher repression capacity (Gatti-Lafranconi, et al., 2013). We tested the three repressors (3R) genetic switch integrated in the chromosome of SIEC and tuned its performance with different RBS and protein degradation signals controlling the levels and half-life of $LacI^{W220F}$. The optimized 3R switch is a highly efficient regulatory module that minimizes leakiness of the *Ptac* promoters and boosts expression of T3SS injectisomes in SIEC strain upon aTc induction. Given the common use of the *Ptac* promoter for expression of heterologous proteins in *E. coli*, the 3R switch has the potential to be applied beyond SIEC strain. Further, its modularity and tunability could also enable replacement of TetR by other repressors to control *Ptac* promoters with alternative inducers.

Results

Design of the 3R genetic switch for tight control of *Ptac* promoters in SIEC. To change the inducer of the T3SS injectisome to aTc and to achieve a tight control of its expression in SIEC, we designed the 3R switch that controls the levels of LacI (Figure 1B). In SIEC, the endogenous LacI encoded by *E. coli* K-12 is not able to fully repress

the *Ptac* promoters controlling the integrated eLEE operons, resulting in the leakiness of T3SS components in the absence of IPTG (Ruano-Gallego, et al., 2015). Therefore, we first deleted the endogenous *lacI* gene in SIEC and use the more repressive LacI^{W220F} variant in the 3R switch. The mutation W220F in LacI confers increased affinity for its DNA operator and reduces binding to IPTG, resulting in a ~10-fold reduction in leakiness in *lac* promoters (Gatti-Lafranconi, et al., 2013). The gene *lacI^{W220F}* was placed under the control of the strong promoter P_R from lambda bacteriophage, which is controlled by the cI repressor (Oppenheim, et al., 2005). This repressor is cleaved by autoproteolysis during the *E. coli* SOS response to DNA damage (Maslowska, et al., 2019). To avoid this phenomenon, we employed a cI variant less susceptible to autoproteolysis due to its E118K mutation, called cI ind- (Gimble and Sauer, 1986). The expression of cI ind- was placed under the *Ptet* promoter and its repressor TetR, which is controlled by the inducer aTc (Bertram and Hillen, 2008, Bertram, et al., 2022). The location of these genetic elements in the 3R circuit is depicted in Figure 1B. A strong RBS (0030) (http://parts.igem.org/Part:BBa_B0030) was utilized for translation of the genes *cI ind-* and *lacI^{W220F}*. Transcriptional terminators T0 (http://parts.igem.org/Part:BBa_B0010) and T1 (http://parts.igem.org/Part:BBa_K864600) were placed downstream of *tetR* and *cI ind-* genes, respectively. Every component of the 3R genetic switch was engineered in a modular way, so that each part (including RBS and terminators) could be easily exchanged. This first version of the 3R regulatory switch was named 3R-I. The whole system was expected to be derepressed with aTc, which binds to TetR freeing the *Ptet* promoter for the expression of cI ind-. This repressor acts over the promoter P_R inhibiting the transcription of *lacI^{W220F}*. Consequently, the LacI^{W220F} levels in the cell should drop allowing transcription from *Ptac* promoters in the eLEE operons (Figure 1B).

To test the functionality of the 3R-I switch, this genetic module was integrated in the chromosome of SIEC at the curli locus (*csg*) (Barnhart and Chapman, 2006), thus generating the strain SIEC-I (Table 1; Experimental procedures). The expression levels of LacI^{W220F} were determined by western blot in whole-cell protein extracts from cultures

of SIEC-I, SIEC, and SIEC∆*lacI* strains, in the presence or absence of inducers (i.e., IPTG or aTc) (Figure 2). The SIEC∆*lacI* strain was used as a control since it lacks LacI and consequently, T3SS components are constitutively expressed. This experiment revealed that the endogenous levels of LacI in SIEC were insufficient for western blot detection with the anti-LacI antibody under our experimental conditions (Figure 2, LacI panel). In contrast, in the absence of aTc, a protein band corresponding to $LacI^{W220F}$ was clearly visible in the SIEC-I strain, which indicated its high expression levels from the P_R promoter in the 3R switch. When aTc was added to the culture of SIEC-I, $LacI^{W220F}$ levels were strongly downregulated and became hardly detectable, which suggested that derepression of TetR with aTc induced sufficient cI ind- levels to repress the transcription of $lacI^{W220F}$. Detection of the cytoplasmic chaperonin GroEL in these protein extracts was used as internal loading control (Figure 2, GroEL panel). These data indicated that the genetic elements of the 3R-I switch and their basic interactions behave as predicted.

Next, we used specific antibodies against the T3SS components EscC, EspA and EspB to detect these proteins by western blot in whole-cell protein extracts or supernatants (secreted proteins) from these bacterial cultures (Figure 2). The genes encoding these T3SS components are in two different eLEE operons: *escC* in eLEE2; *espA* and *espB* in eLEE4 (Figure 1B). EscC assembles the OM secretin, an essential structural component of the injectisome (Figure 1A) (Ogino, et al., 2006). EspA forms a long extracellular filament of the injectisome (Sekiya, et al., 2001, Zheng, et al., 2021) to which EspB associates to assemble the translocon pore in the host cell membrane (Figure 1A) (Hartland, et al., 2000, Iizumi, et al., 2007, Luo and Donnenberg, 2011). Detection of extracellular translocon proteins EspA and EspB implies that the injectisome is correctly assembled and functional, since their secretion is mediated by an active needle complex (Gaytan, et al., 2016).

As expected from previous work, EspA, EspB and EscC proteins were detectable in SIEC in the absence of IPTG due to leaky expression (Figure 2). This was more evident

for EscC in whole-cell extracts, but it was also clearly observed for secreted EspA and EspB. When IPTG was added to the SIEC culture, expression of these T3SS components was upregulated (Figure 2). In the case of SIECΔ*lacI* strain, these T3SS proteins were constitutively expressed regardless of the presence of IPTG. Contrary to these strains, a strong repression of T3SS components was found in SIEC-I in the absence of the inducer, which was in good agreement with the high levels of $LacI^{W220F}$ in this strain. However, addition of aTc did not derepress this strain, since secreted EspA and EspB were not detected in culture supernatants and only a faint protein band of EscC was found in whole-cell extracts (Figure 2). This result indicated that the 3R-I circuit was not capable of upregulating the eLEE operons to levels sufficient for the assembly of active injectisomes. Addition of IPTG to directly derepress $LacI^{W220F}$ was also not effective for the assembly of injectisomes in SIEC-I (Figure 2), likely because of the high levels of $LacI^{W220F}$ and the low affinity of this mutant repressor for IPTG (Gatti-Lafranconi, et al., 2013).

Tuning $LacI^{W220F}$ levels with ssrA protein degradation and translation initiation regions. The above results suggested that the low levels of $LacI^{W220F}$ present in SIEC-I with aTc were sufficient to repress the eLEE operons. This pointed out the necessity to optimize the 3R-I circuit to further decrease $LacI^{W220F}$ protein levels upon aTc induction for an effective expression of the eLEE operons. To this end, we fused ssrA protein degradation tags -LAA, -AAV and -ASV to the C-terminal end of $LacI^{W220F}$ (Karzai, et al., 2000). These degradations tags decrease GFP half-life in *E. coli* from ~ 225 min to 40 min (-LAA tag), 60 min (-AAV tag) or 110 min (-ASV tag) (Andersen, et al., 1998). The genes encoding $LacI^{W220F}$ with -LAA, -AAV and -ASV tags were inserted in the 3R circuit replacing the original $lacI^{W220F}$ gene, thus generating switches 3R-LAA, 3R-AAV, and 3R-ASV, respectively. These 3R switches were integrated in the *csg* locus of SIEC generating SIEC-L (with 3R-LAA), SIEC-A (with 3R-AAV) and SIEC-X (with 3R-ASV) strains (Table 1). The capacity of these SIEC strains to control the expression of the eLEE operons was compared to the parental SIEC and SIEC-I strains using western blot

to detect LacI^{W220F}, EscC, EspB and EspA proteins (Figure 3A). As before, high levels of LacI^{W220F} were found in the uninduced SIEC-I, which showed almost no expression of T3SS components (OFF state). In contrast, in the uninduced cultures of SIEC-L and SIEC-A the LacI^{W220F} repressor was not detected, and a strong leakiness of T3SS components was found. These results pointed that the tags -LAA and -AAV effectively degraded LacI^{W220F} in SIEC-L and SIEC-A bacteria. In contrast, LacI^{W220F} was detectable in the uninduced SIEC-X cultures, which carried the weakest degradation tag tested (-ASV). Interestingly, the lower levels of LacI^{W220F} in SIEC-X were sufficient to maintain a repressed OFF state with little leakiness and to induce the expression of T3SS components when aTc was added (ON state), with expression levels slightly lower compared to those produced by the parental SIEC in the presence of IPTG (Figure 3A). Consequently, the LacI^{W220F} with the ssrA tag -ASV appeared to maintain repression (OFF state) while not greatly compromising the activation of the system with aTc (ON state).

We attempted to improve the 3R-X switch to further enhance expression in the ON state. To this end, we generated versions with lower expression of LacI^{W220F}-ASV using weaker ribosome binding sites (RBS). The RBS 0034 (http://parts.igem.org/Part:BBa_B0034) was used for translation of LacI^{W220F}-ASV generating 3R-X2 variant and the strain SIEC-X2 upon integration in *csg* locus. In addition, the RBS 0034 was combined with the weak start codon GTG (Hecht, et al., 2017) to generate the 3R-X3 switch and the resulting strain SIEC-X3 (Table 1). When testing the performance of these new versions, a gradual decrease in the LacI^{W220F} expression levels was detected (SIEC-I > SIEC-X > SIEC-X2 > SIEC-X3) (Figure 3B). However, the reduction of LacI^{W220F} levels in these strains had little impact on the expression of T3SS components upon induction, with just a moderate increase detectable in SIEC-X3, but also with a similar parallel increase in the leakiness of the system (Figure 3B). This scenario suggested that further reductions in the levels of LacI^{W220F} in SIEC-X compromised the OFF state.

Optimizing the 3R switch with the orthogonal protease *mf*-Lon. We explored an alternative approach to balance the levels of LacI^{W220F} in the ON state without compromising the OFF state. To this end, a new orthogonal element was introduced in the 3R circuit: the Lon protease from *Mesoplasma florum* (*mf*-Lon) (Cameron and Collins, 2014). This protease recognizes a specific ssrA-tag of *M. florum* (*mf*-ssrA) at the C-terminal end of the target protein. The *mf*-ssrA tag is not recognized by the endogenous Lon protease of *E. coli*, which makes *mf*-Lon an effective orthogonal protein degradation system independent of the *E. coli* protein degradation (Moser, et al., 2018). Interestingly, a previous study had reported the use of *mf*-Lon to downregulate the pool of wild-type LacI in *E. coli* as part of a genetic circuit controlling expression of toxins (Chan, et al., 2016). Based on the first version of the circuit, 3R-I, the *mf*-Lon protease coding gene was placed downstream the *cI ind-* gene, in a bicistronic configuration controlled by the *tet* promoter. The *mf*-ssrA tag sequence was fused to the C-terminal part of the LacI^{W220F} protein. With this new version, named 3R-XLon, the LacI^{W220F} repressor with *mf*-ssrA tag would be produced at high levels when the inducer aTc is not present. Upon aTc induction, both the repressor cI and the *mf*-Lon would be produced, blocking the transcription of *lacI^{W220F}* and degrading the remaining LacI^{W220F} protein (Figure 4A). This might result in an effective depletion of LacI^{W220F}, rendering a complete activation in ON state without affecting the repression in OFF state.

As with previous versions, the 3R-XLon switch was integrated in the *csg* site of SIEC. The resulting strain, SIEC-XLon (Table 1), was analyzed by western blot to determine LacI levels and its capacity to regulate the expression of the T3SS components (Figure 4B). The SIEC-XLon was compared with the strains SIEC-I (first version) and SIEC-X (with -ASV tag fused to LacI^{W220F}), and the parental SIEC strain and the unrepressed mutant SIECΔ*lacI* were used as additional controls. The newly engineered strain SIEC-XLon showed high expression of the repressor LacI^{W220F} with *mf*-ssrA tag in the OFF

state, at similar levels than the ASV-tagged LacI^{W220F} in SIEC-X, but lower than LacI^{W220F} without any tag in SIEC-I (Figure 4B). This decrease of LacI^{W220F} levels with the *mf*-Lon tag could be due to some leaky expression of the *mf*-Lon protease in the OFF state. Nevertheless, the amount of LacI^{W220F} in the OFF state was enough to keep good repression levels of the T3SS components, also indicating that the *mf*-ssrA tag did not impair the functionality of LacI^{W220F}. The levels of the different versions of LacI/ LacI^{W220F} and EscC in the bacterial cell, and those of EspA and EspB in the culture supernatants, were quantified from the western blot signals (Figure 5). In SIEC-XLon almost no secretion of EspA nor EspB was detected in the OFF state (Figure 5A and 5B) and the leakiness of EscC expression was significantly reduced in comparison with the parental SIEC and SIEC-X strains, being similar to SIEC-I (Figure 5C). Therefore, the strain SIEC-XLon showed a tight control of the system in the OFF state. When the system was induced with aTc, the LacI^{W220F} repressor in SIEC-XLon was no longer detected (Figure 5D), whereas secreted EspA and EspB and cellular EscC were in higher amounts than in the previous SIEC strains (Figure 5A, 5B, and 5C). We determined a 3 to 4-fold increase in the expression of these T3SS proteins in SIEC-XLon compared to the parental SIEC, indicating that the ON state was boosted with this version of the genetic circuit. The degradation of the remaining LacI^{W220F} by the *mf*-Lon protease after induction appears crucial to achieve this efficient induction of the system. Importantly, the increased amounts of EspB and EspA detected in the culture supernatant of SIEC-XLon cultures in ON state indicated that higher expression of the T3SS operons resulted in a higher assembly of functional injectisomes in this strain. This was also confirmed by SDS-PAGE analysis of concentrated supernatants of induced cultures of the strains SIEC, SIEC-I, SIEC-X and SIEC-XLon (Figure 4C). After Coomassie staining, protein bands corresponding to EspA and EspB (along with EspD) were observed in induced culture supernatants of the four strains. Nevertheless, in agreement with the western blot results the amount of these proteins was much higher in SIEC-XLon than in any other

SIEC strains. Overall, these results indicated that in SIEC-XLon the system was fully repressed in the OFF state and efficiently induced in the ON state.

Comparison of the 3R switches performance using a *gfp* reporter. We further characterized the performance of the 3R switches by analyzing the expression of a heterologous reporter protein (GFP) under the control of the *Ptac* promoter. A gene fusion between the *Ptac* and a codon-optimized *gfp* variant (Corcoran, et al., 2010) was integrated in the chromosomal locus *ypjA* (Roux, et al., 2005, Vo, et al., 2017) of the strains SIEC, SIEC-I, SIEC-X and SIEC-XLon. The production of GFP was determined in the resulting strains (Table 1) as fluorescence normalized per OD_{600} after 6 h, 12 h, and 18 h induction in static culture conditions (Figure 6A). In the absence of the inducer (OFF state), the strain SIEC-GFP presented the highest leakiness of GFP expression among all strains. As expected, SIEC-I-GFP showed almost no leakiness, but GFP was not induced upon addition of aTc. SIEC-X-GFP behavior was more balanced, with a clear induction of GFP with aTc, close to that of the parental SIEC with IPTG, but with reduced leakiness in the absence of aTc. Notably, SIEC-XLon-GFP showed tight control of GFP expression in the OFF state, similar to SIEC-I-GFP, but with a strong GFP expression when induced with aTc (ON state) (Figure 6A). These results were in line with the observed expression of the T3SS components, where the 3R circuit in SIEC-XLon had the best performance in both OFF and ON states.

We determined the dynamic range of the 3R switches, defined as the difference between the signal (induced) and the background noise (non-induced), and calculated by subtracting in each timepoint the detected signal without inducer to the signal when the inducer is present. By using this, genetic circuits can be easily compared in terms of expression *versus* leakiness (ON *vs*. OFF). The different SIEC strains with the GFP reporter were grown in parallel and incubated in the presence or absence of the corresponding inducer. GFP expression was monitored continuously along the time as fluorescence normalized per OD_{600} (Figure 6B). As could be anticipated, the first version

of the circuit (SIEC-I-GFP) showed a constant low dynamic range, presenting no variation between ON/OFF states along the time, and confirming that this version cannot be induced. The original strain SIEC-GFP, with the endogenous LacI regulation, and the strain SIEC-X-GFP presented medium values of dynamic range, but the latter was able to induce the GFP expression faster. Finally, the optimized strain SIEC-XLon-GFP showed the best performance in dynamic range, presenting the highest fluorescence values and a steady increase along the time, indicating that a strong induction was occurring while also being able to maintain an efficient OFF state (Figure 6B). Thus, this demonstrates the genetic circuit incorporated in SIEC-XLon is able to efficiently regulate the expression of *Ptac-gfp* and of the T3SS operons.

Bacterial growth with 3R switches in OFF and ON states. Lastly, we studied the growth of the different bacterial strains with 3R switches in OFF and ON states, when inducing expression of T3SS proteins and GFP. Noticeably, the insertion of the different 3R circuit versions did not interfere in bacterial growth since all the strains showed similar growth curves in non-induced OFF state (Figure 6C). Although no significant differences in growth rate between OFF and ON states were observed in exponential phase, the final OD_{600} reached by the cultures at stationary phase was reduced in the ON state for all strains. The magnitude of this reduction inversely correlated to the levels of expression of the T3SS components, being the growth of SIEC-XLon the most affected in the ON state (~40% reduction in final OD_{600}) and SIEC-I the less affected (~7%). The final OD_{600} of SIEC and SIEC-X in the ON state were similar, with a reduction of final OD_{600} ~20% compared to the OFF state. This suggests that induction of the T3SS proteins (and GFP) represented a burden on the growth of these strains. Nevertheless, the changes in the maximum OD_{600} of the induced cultures were not severe for SIEC and SIEC-X strains and were only significant for the overexpressing SIEC-XLon strain. Importantly, in all cases, changes in growth only occurred in the induced ON state, assuring good bacterial growth of all SIEC strains (even those with leakiness) before T3SS induction.

Discussion

We have demonstrated that the 3R circuit reported in this work allows a tight control of the expression of multiple *Ptac* promoters integrated in the chromosome of *E. coli*. Use of the 3R switch minimizes the leakiness of the *lacI*-*Plac*/*Ptac* system (Wilson, et al., 2007) in the OFF state and maximizes its induction in the ON state. To design the 3R circuit we have followed the basic principles to assemble a genetic circuit with interconnected genetic parts (Voigt, 2006, Brophy and Voigt, 2014). The TetR repressor was used to tightly control expression of lambda cI (ind-) repressor (and *mf*-Lon in the XLon version) with the inducer aTc (Bertram and Hillen, 2008, Bertram, et al., 2022). The use of the strong lambda P_R promoter (Oppenheim, et al., 2005) to drive expression of the $LacI^{W220F}$ allowed us to have high levels of this highly active LacI repressor mutant in the OFF state (Gatti-Lafranconi, et al., 2013). The efficient repression of lambda P_R by cI (ind-) (Sauer, et al., 1982, Gimble and Sauer, 1986) dramatically downregulated $LacI^{W220F}$ levels in the ON state. However, the low amounts of $LacI^{W220F}$ remaining in the bacterium upon aTc induction needed to be further reduced by proteolysis (Karzai, et al., 2000) to enable induction of the *Ptac* promoters. This was first achieved in the 3R-X version by incorporating a C-terminal ASV ssrA tag (Andersen, et al., 1998) recognized by the endogenous *E. coli* proteolysis system, which showed reduced $LacI^{W220F}$ levels in both OFF and ON states. A better digital behavior of the switch in OFF and ON states was obtained in the 3R-XLon version, by incorporating the orthogonal *mf*-Lon protease (Cameron and Collins, 2014) downstream of cI (ind-) gene, and the C-terminal *mf*-ssrA tag fused to $LacI^{W220F}$. Using this approach, the levels of $LacI^{W220F}$ were only reduced by proteolysis upon induction of *mf*-Lon protease in the ON state. Thus, simultaneous expression of cI (ind-) and *mf*-Lon in the 3R-XLon switch ensures both inhibition of transcription of *lacI*^{W220F} gene and proteolysis of the pool of $LacI^{W220F}$ in the bacterium.

We have demonstrated the utility of the 3R genetic circuit to control the assembly of a macromolecular complex injectisome engineered in the SIEC strain (Ruano-Gallego, et al., 2015). The regulation implemented by the 3R switches -X and -XLon improves the original induction mechanism of the SIEC strain by reducing leakiness in the OFF state while enabling sufficient expression of the T3SS components for injectisome assembly in the ON state. The 3R switch allows the use of aTc as inducer, which is suitable for *in vivo* administration (Loessner, et al., 2009, Kotula, et al., 2014) unlike IPTG (Wyborski and Short, 1991). Upon addition of aTc, the SIEC-X and SIEC-XLon strains produce the components of the T3SS and assemble functionally active injectisomes as determined by the secretion of EspA and EspB proteins. Thus, these strains could be induced with aTc for delivery of therapeutic protein *in vivo*. The expression of the T3SS injectisomes and the dynamic range (ON *vs*. OFF) were maximal in the induced SIEC-XLon strain, which carries the orthogonal protein degradation system. The high levels of T3SS proteins produced by SIEC-XLon upon induction likely entail a burden on the growth of this strain with aTc. The burden of T3SS expression is less evident for the SIEC-X strain, which grows similarly than the original SIEC strain. Nevertheless, the tight control of the injectisome expression exerted by the 3R regulatory circuit enables the optimal propagation of both SIEC-X and SIEC-XLon in the OFF state before induction. This expression control will contribute to the safety and potential effectiveness of these strains for developing living therapeutics (Piñero-Lambea, et al., 2015, Ozdemir, et al., 2018, Riglar and Silver, 2018).

Therefore, the reported 3R switches can be an effective general tool to control the expression of heterologous proteins under *lac* and *tac* promoters in *E. coli* and other bacteria (Camsund, et al., 2014, Rosano and Ceccarelli, 2014), with minimal expression leakiness and maximal expression levels, allowing the use of aTc instead of IPTG for induction. The modularity of the 3R switch could also enable the use of other inducers by a single modification, replacing the TetR-*Ptet* module with a different regulatory element that could respond to other inducers or environmental cues found *in vivo* (e.g.,

inflammatory molecules) (Riglar and Silver, 2018). The modularity of the circuit further allows the use of other promoters besides *Ptac*, provided the corresponding repressor is placed in substitution of LacI within the 3R construct. Alternatively, hybrid synthetic promoters with engineered LacI operators (*lac*O) (Schuller, et al., 2020) could be controlled by LacI in the current configuration of the 3R switch.

Conclusions

We have reported the design, construction, validation and optimization of the genetic circuit 3R based on three repressors (TetR, cI ind-, and $LacI^{W220F}$) that allows efficient and simultaneous control of the expression of multiple *Ptac* promoters integrated in the chromosome of *E. coli*. The 3R switch was tuned in distinct versions using different genetic parts (e.g., RBS) and SsrA protein degradation signals, endogenous or orthogonal to *E. coli* (Cameron and Collins, 2014). The optimized versions can control the expression of *Ptac* promoters with nearly digital (OFF/ON) behavior by the addition of the inducer aTc. Implementation of 3R circuit in the engineered SIEC strain (Ruano-Gallego, et al., 2015) enabled the effective repression of *Ptac* promoters in the OFF state and their induction in the ON state to sufficient levels to assemble functional T3SS injectisomes. The presence of the 3R switches did not alter bacterial growth in the OFF state, ensuring good bacterial growth of the engineered *E. coli* strains before induction. The highest level of induction in the ON state was obtained with the optimized 3R-XLon version, which induces the *mf*-Lon protease to degrade $LacI^{W220F}$. Overexpression of the T3SS in this strain also imposed a higher burden for the growth of the induced bacteria. The 3R switch can be used as a general genetic tool to tightly control expression of heterologous proteins under *lac* and *tac* promoters in *E. coli* and other bacteria.

Experimental procedures

Bacterial growth conditions. Strains of bacteria used in this work are listed in Table 1. Bacteria were grown in Lysogenic Broth (LB) medium (Miller, 1992) at 37 ºC with shaking (160 rpm), unless otherwise indicated. For solid media, agar was added to LB (1.5% w/v). When needed for selection purposes, antibiotics were added at the following concentrations: kanamycin (Km) at 50 µg/ml and spectinomycin (Sp) at 50 µg/ml.

Plasmid constructs and strain engineering. The plasmids used in the present study are listed in Table 2**.** Plasmids were constructed following standard restriction enzyme-based genetic engineering (Ausubel, et al., 2002). Restriction enzymes were obtained from New England Biolabs and Thermo Fisher Scientific. The DNA encoding the original circuit (3R-I) was obtained by gene synthesis (GeneArt, Thermo Fisher Scientific). DNA amplifications for cloning were carried out by the proofreading DNA polymerase Herculase II Fusion (Agilent Technologies), followed by an isolation step in agarose gel by size. Oligonucleotides used as primers (Supplementary Table S1) were ordered from Sigma-Aldrich. Ligation of plasmid backbone and insert was catalyzed in an overnight reaction using the T4 DNA ligase (Roche). All generated constructs were first screened for the presence of the insert by PCR amplification using NZYProof 2x Green Master Mix (NZYtech) and the selected plasmid constructs were sequenced by Sanger chain-terminator method (Macrogen). For cloning and propagation of suicide pGE-plasmid derivatives (Piñero-Lambea, et al., 2015), containing the conditional pi-dependent R6K origin of replication (Stalker, et al., 1982), the *E. coli* strain BW25141 was employed (Datsenko and Wanner, 2000). Details of plasmid construction can be found in the Supporting information.

The *E. coli* strains engineered for this work are listed in Table 1. Site-specific deletions and insertions in the chromosome of *E. coli* were performed based on homologous recombination with pGE-suicide plasmids and the resolution of cointegrants by expression of I-SceI endonuclease (Posfai, et al., 1999, Posfai, et al., 2006) leaving no

antibiotic resistance marker or scars in the chromosome, as described previously (Piñero-Lambea, et al., 2015). Briefly, the *E. coli* strain to be modified was initially transformed with plasmid pACBSR (Sp^R variant) (Ruano-Gallego, et al., 2015), expressing I-SceI and λ Red proteins under the control of the *bad* promoter (inducible by L-arabinose) (Herring, et al., 2003), and subsequently electroporated with the corresponding pGE-based suicide vector (Km^R). Cointegrants were selected on LB-Sp-Km plates incubated at 37°C. Individual colonies were grown for 6 h in LB-Sp liquid medium containing ARA, (L-arabinose at 0.4% w/v) at 37 ºC with agitation (160 rpm). After this period, the culture was streaked on LB-Sp plates using an inoculating loop and incubated overnight. Individual colonies were replicated in LB-Sp along with LB-Sp-Km to screen for Km-sensitive colonies that have performed resolution of the cointegrant vector after I-SceI induction. Individual Km-sensitive colonies were screened by PCR with specific oligonucleotides to identify those with the desired modification in their chromosome (i.e., deletion, insertion, substitution). In some cases bacterial chromosomal DNA was also isolated and the integrated 3R switch amplified with the proofreading DNA polymerase Herculase II Fusion, followed by agarose gel purification of the corresponding amplicon for DNA sequencing with specific primers (Macrogen).

Injectisome expression in SIEC derived strains. For induction of SIEC strains for analysis of the T3SS components and LacI/$LacI^{W220F}$ expression, bacteria were grown overnight from a single colony with shaking (160 rpm) at 37 ºC. Next day, cultures were diluted 1:100 in 5 ml of LB with the appropriate T3SS inducer (IPTG at 0.1mM or aTc at 50 ng/ml), in capped Falcon tubes (BD Biosciences), and incubated for 6 h under the same conditions. Induced bacteria were harvested by centrifugation at 4000 rpm for 15 min, and bacterial pellet and supernatant fractions were split and processed separately. Pellet samples were washed in PBS 1X (phosphate-buffered saline: 8 mM Na_2HPO_4, 1.5 mM KH_2PO_4, 3 mM KCl, 137 mM NaCl pH 7.0) and concentrated 10 times before boiling

with reducing loading buffer [60 mM Tris-HCl pH 6.8, 1% (w/v) SDS, 5% (v/v) glycerol, 0.005% (w/v) bromophenol blue and 1% (v/v) 2-mercaptoethanol] for 10 min. Supernatant fraction was centrifuged 3 times for eliminating bacterial remnants and directly boiled with reducing loading buffer for 10 min. If concentrated, the supernatant was chilled on ice and incubated 60 min with trichloroacetic acid (TCA, Merck) at 20% w/v for precipitation of proteins. After cold centrifugation (20000g, 15 min), TCA-precipitated protein pellets were rinsed with cold acetone (-20ºC) and resuspended in PBS before boiling with reducing loading buffer for 10 min. The different samples in loading buffer were analyzed by SDS-PAGE and/or western-blot as described below.

SDS-PAGE and western Blot. Sodium Dodecyl Sulfate-Polyacrylamide gel electrophoresis (SDS-PAGE) was used for analysis of proteins after the expression assays (Ausubel, et al., 2002). Electrophoresis was carried out on 15 % polyacrylamide SDS gels following standard methods using the Miniprotean III system (Bio-Rad). Once separated by SDS-PAGE, proteins were either stained with Coomassie Blue R-250 (Bio-Rad) or transferred to a polyvinylidene difluoride membrane (PVDF, Immobilon-P Milipore) for western blot analysis. This transference was performed by semi-dry electrophoresis system (Bio-Rad). Antibodies used are indicated in the Supplementary Table S2. Membranes were developed with the western ECL Substrate kit (Bio-Rad) and images were acquired using a ChemiDoc Touch system (Bio-Rad).

Quantification of T3SS proteins and LacI/LacI^{W220F} was performed by densitometry using the ImageLab® software (BioRad) from three independent experiments. Signal values were calculated as a percentage, taking as 100 % the expression levels of induced SIEC strain in the case of the T3SS proteins and non-induced SIEC-I in the case of LacI/LacI^{W220F} repressor.

GFP expression assay. GFP expression was determined by on-plate quantification of fluorescence during bacterial growth with and without inducer. For that purpose,

overnight bacterial cultures grown at 37 ºC in static conditions were diluted 1/100 in LB medium and incubated for 2 h under the same conditions. Bacterial cultures were diluted to 0.1 OD_{600} and placed into 96-well black plates with flat clear bottom (Corning) adding the corresponding inducer when indicated (IPTG at 0.1 mM or aTc at 50 ng/ml). Normalized fluorescence determination during growth was quantified by continued readings in a Victor-2 multireader spectrophotometer (Perkin Elmer). The cultures were incubated at 30°C with rotatory shaking, while growth (OD_{600}) and GFP fluorescence were recorded every 15 min. Each reading was normalized by OD_{600} for each timepoint. The dynamic range at each time point was calculated by subtracting the normalized GFP expression of non-induced cultures from the value of induced cultures. Represented data for GFP expression, dynamic range and strain growth was the mean from three independent experiments.

SBOL diagrams. All diagrams representing the genetic constructs and their interactions showed in this work were drawn using the guidelines and standardized visual glyphs from the Synthetic Biology Open Language, SBOL visual (Galdzicki, et al., 2014, Quinn, et al., 2015) (sbolstandard.org).

Acknowledgements

We thank Dr. Belén Calles and Dr. Esteban Martínez (CNB-CSIC) for assistance in the quantification of GFP expression.

Funding

This work was supported by the following Research Grants to L.A.F.: MCIN/AEI and FEDER BIO2017-89081-R, MCIN/AEI and NextGeneration EU/ PRTR (PLEC2021-007739), and the European Union's Horizon 2020 Future and Emerging Technologies research and innovation program (FET Open 965018-BIOCELLPHE). This work was also supported by PhD contracts FPI BES-2015-073850 to A.A.C., FPU16/01427 to A.C.M.; and FPU18/03199 to A.M.P.

Author contributions

Alejandro Asensio-Calavia: Conceptualization (equal); data curation (lead); formal analysis (lead); investigation (lead); methodology (lead); visualization (lead); validation (supporting); writing – original draft (equal); writing – review and editing (supporting).

Álvaro Ceballos-Munuera: Conceptualization (equal); data curation (supporting); formal analysis (supporting); investigation (supporting); methodology (supporting); validation (supporting); visualization (supporting); writing – review and editing (supporting).

Álmudena Méndez-Pérez: Conceptualization (equal); formal analysis (supporting); investigation (supporting); validation (supporting); visualization (supporting); writing – review and editing (supporting).

Beatriz Álvarez: Conceptualization (equal); formal analysis (supporting); investigation (supporting); methodology (supporting); supervision (supporting); validation (supporting); writing – original draft (equal); visualization (supporting); writing – review and editing (supporting).

Luis Ángel Fernández: Conceptualization (equal); funding acquisition (lead); formal analysis (supporting); methodology (supporting); resources (lead); supervision (lead); validation (lead); visualization (supporting); writing – review and editing (equal).

Competing interests

The authors declare that they have no competing interests.

References

Andersen, J.B., Sternberg, C., Poulsen, L.K., Bjorn, S.P., Givskov, M., and Molin, S. (1998) New unstable variants of green fluorescent protein for studies of transient gene expression in bacteria, *Appl Environ Microbiol* **64**: 2240-2246.

Ausubel, F.M., Brent, R., Kingston, R.E., Moore, D.D., Seidman, J.G., Smith, J.A., and Struhl, K. (2002) *Short Protocols in Molecular Biology*. New York: John Wiley & Sons, Inc.

572 Bai, F., Li, Z., Umezawa, A., Terada, N., and Jin, S. (2018) Bacterial type III secretion
573 system as a protein delivery tool for a broad range of biomedical applications,
574 *Biotechnol Adv* **36**: 482-493.

575 Barnhart, M.M., and Chapman, M.R. (2006) Curli biogenesis and function, *Annu Rev*
576 *Microbiol* **60**: 131-147.

577 Berens, C., and Hillen, W. (2003) Gene regulation by tetracyclines. Constraints of
578 resistance regulation in bacteria shape TetR for application in eukaryotes, *Eur J*
579 *Biochem* **270**: 3109-3121.

580 Bertram, R., and Hillen, W. (2008) The application of Tet repressor in prokaryotic gene
581 regulation and expression, *Microb Biotechnol* **1**: 2-16.

582 Bertram, R., Neumann, B., and Schuster, C.F. (2022) Status quo of tet regulation in
583 bacteria, *Microb Biotechnol* **15**: 1101-1119.

584 Blanco-Toribio, A., Muyldermans, S., Frankel, G., and Fernández, L.A. (2010) Direct
585 injection of functional single-domain antibodies from *E. coli* into human cells, *PLoS*
586 *One* **5**: e15227.

587 Brooks, S.M., and Alper, H.S. (2021) Applications, challenges, and needs for
588 employing synthetic biology beyond the lab, *Nat Commun* **12**: 1390.

589 Brophy, J.A., and Voigt, C.A. (2014) Principles of genetic circuit design, *Nat Methods*
590 **11**: 508-520.

591 Butan, C., Lara-Tejero, M., Li, W., Liu, J., and Galan, J.E. (2019) High-resolution view
592 of the type III secretion export apparatus in situ reveals membrane remodeling and a
593 secretion pathway, *Proc Natl Acad Sci U S A* **116**: 24786-24795.

594 Cameron, D.E., and Collins, J.J. (2014) Tunable protein degradation in bacteria, *Nat*
595 *Biotechnol* **32**: 1276-1281.

596 Camsund, D., Heidorn, T., and Lindblad, P. (2014) Design and analysis of LacI-
597 repressed promoters and DNA-looping in a cyanobacterium, *Journal of biological*
598 *engineering* **8**: 4.

599 Chan, C.T., Lee, J.W., Cameron, D.E., Bashor, C.J., and Collins, J.J. (2016) 'Deadman'
600 and 'Passcode' microbial kill switches for bacterial containment, *Nature chemical*
601 *biology* **12**: 82-86.

602 Chopra, I., and Roberts, M. (2001) Tetracycline antibiotics: mode of action,
603 applications, molecular biology, and epidemiology of bacterial resistance, *Microbiol Mol*
604 *Biol Rev* **65**: 232-260 ; second page, table of contents.

605 Corcoran, C.P., Cameron, A.D., and Dorman, C.J. (2010) H-NS silences gfp, the green
606 fluorescent protein gene: gfpTCD is a genetically Remastered gfp gene with reduced
607 susceptibility to H-NS-mediated transcription silencing and with enhanced translation, *J*
608 *Bacteriol* **192**: 4790-4793.

609 Costa, T.R., Felisberto-Rodrigues, C., Meir, A., Prevost, M.S., Redzej, A., Trokter, M.,
610 and Waksman, G. (2015) Secretion systems in Gram-negative bacteria: structural and
611 mechanistic insights, *Nat Rev Microbiol* **13**: 343-359.

612 Cubillos-Ruiz, A., Guo, T., Sokolovska, A., Miller, P.F., Collins, J.J., Lu, T.K., and Lora,
613 J.M. (2021) Engineering living therapeutics with synthetic biology, *Nat Rev Drug Discov*
614 **20**: 941-960.

615 Datsenko, K.A., and Wanner, B.L. (2000) One-step inactivation of chromosomal genes
616 in *Escherichia coli* K-12 using PCR products, *Proc Natl Acad Sci U S A* **97**: 6640-6645.

617 de Boer, H.A., Comstock, L.J., and Vasser, M. (1983) The *tac* promoter: a functional
618 hybrid derived from the *trp* and *lac* promoters, *Proc Natl Acad Sci U S A* **80**: 21-25.

619 Deng, W., Marshall, N.C., Rowland, J.L., McCoy, J.M., Worrall, L.J., Santos, A.S., et al.
620 (2017) Assembly, structure, function and regulation of type III secretion systems, *Nat*
621 *Rev Microbiol* **15**: 323-337.

622 Dvorak, P., Chrast, L., Nikel, P.I., Fedr, R., Soucek, K., Sedlackova, M., et al. (2015)
623 Exacerbation of substrate toxicity by IPTG in *Escherichia coli* BL21(DE3) carrying a
624 synthetic metabolic pathway, *Microb Cell Fact* **14**: 201.

625 Galan, J.E., and Wolf-Watz, H. (2006) Protein delivery into eukaryotic cells by type III
626 secretion machines, *Nature* **444**: 567-573.

627 Galdzicki, M., Clancy, K.P., Oberortner, E., Pocock, M., Quinn, J.Y., Rodriguez, C.A.,
628 et al. (2014) The Synthetic Biology Open Language (SBOL) provides a community
629 standard for communicating designs in synthetic biology, *Nat Biotechnol* **32**: 545-550.

630 Gatti-Lafranconi, P., Dijkman, W.P., Devenish, S.R., and Hollfelder, F. (2013) A single
631 mutation in the core domain of the *lac* repressor reduces leakiness, *Microb Cell Fact*
632 **12**: 67.

633 Gaytan, M.O., Martinez-Santos, V.I., Soto, E., and Gonzalez-Pedrajo, B. (2016) Type
634 Three Secretion System in Attaching and Effacing Pathogens, *Frontiers in cellular and*
635 *infection microbiology* **6**: 129.

636 Gimble, F.S., and Sauer, R.T. (1986) Lambda repressor inactivation: properties of
637 purified ind- proteins in the autodigestion and RecA-mediated cleavage reactions, *J*
638 *Mol Biol* **192**: 39-47.

639 Hartland, E.L., Daniell, S.J., Delahay, R.M., Neves, B.C., Wallis, T., Shaw, R.K., et al.
640 (2000) The type III protein translocation system of enteropathogenic *Escherichia coli*
641 involves EspA-EspB protein interactions, *Mol Microbiol* **35**: 1483-1492.

642 Hecht, A., Glasgow, J., Jaschke, P.R., Bawazer, L.A., Munson, M.S., Cochran, J.R., et
643 al. (2017) Measurements of translation initiation from all 64 codons in *E. coli*, *Nucleic*
644 *Acids Res* **45**: 3615-3626.

645 Herring, C.D., Glasner, J.D., and Blattner, F.R. (2003) Gene replacement without
646 selection: regulated suppression of amber mutations in *Escherichia coli*, *Gene* **311**:
647 153-163.

648 Hu, J., Worrall, L.J., Vuckovic, M., Hong, C., Deng, W., Atkinson, C.E., et al. (2019)
649 T3S injectisome needle complex structures in four distinct states reveal the basis of
650 membrane coupling and assembly, *Nat Microbiol* **4**: 2010-2019.

651 Iizumi, Y., Sagara, H., Kabe, Y., Azuma, M., Kume, K., Ogawa, M., et al. (2007) The
652 enteropathogenic *E. coli* effector EspB facilitates microvillus effacing and
653 antiphagocytosis by inhibiting myosin function, *Cell Host Microbe* **2**: 383-392.

Ittig, S.J., Schmutz, C., Kasper, C.A., Amstutz, M., Schmidt, A., Sauteur, L., et al. (2015) A bacterial type III secretion-based protein delivery tool for broad applications in cell biology, *J Cell Biol* **211**: 913-931.

Karzai, A.W., Roche, E.D., and Sauer, R.T. (2000) The SsrA-SmpB system for protein tagging, directed degradation and ribosome rescue, *Nat Struct Biol* **7**: 449-455.

Kosinski, M., Rinas, U., and Bailey, J. (1992) Isopropyl-?-d-thiogalactopyranoside influences the metabolism of *Escherichia coli*, *Applied Microbiology and Biotechnology* **36**: 782-784.

Kotula, J.W., Kerns, S.J., Shaket, L.A., Siraj, L., Collins, J.J., Way, J.C., and Silver, P.A. (2014) Programmable bacteria detect and record an environmental signal in the mammalian gut, *Proc Natl Acad Sci U S A* **111**: 4838-4843.

Leventhal, D.S., Sokolovska, A., Li, N., Plescia, C., Kolodziej, S.A., Gallant, C.W., et al. (2020) Immunotherapy with engineered bacteria by targeting the STING pathway for anti-tumor immunity, *Nat Commun* **11**: 2739.

Loessner, H., Leschner, S., Endmann, A., Westphal, K., Wolf, K., Kochruebe, K., et al. (2009) Drug-inducible remote control of gene expression by probiotic *Escherichia coli* Nissle 1917 in intestine, tumor and gall bladder of mice, *Microbes Infect* **11**: 1097-1105.

Luo, W., and Donnenberg, M.S. (2011) Interactions and predicted host membrane topology of the enteropathogenic *Escherichia coli* translocator protein EspB, *J Bacteriol* **193**: 2972-2980.

Maslowska, K.H., Makiela-Dzbenska, K., and Fijalkowska, I.J. (2019) The SOS system: A complex and tightly regulated response to DNA damage, *Environ Mol Mutagen* **60**: 368-384.

Miller, J.H. (1992) *A short course in bacterial genetics: a laboratory manual and handbook for Escherichia coli and related bacteria*. Cold Spring Harbor, New York: Cold Spring Harbor Laboratory Press.

Moser, F., Espah Borujeni, A., Ghodasara, A.N., Cameron, E., Park, Y., and Voigt, C.A. (2018) Dynamic control of endogenous metabolism with combinatorial logic circuits, *Mol Syst Biol* **14**: e8605.

Ogino, T., Ohno, R., Sekiya, K., Kuwae, A., Matsuzawa, T., Nonaka, T., et al. (2006) Assembly of the type III secretion apparatus of enteropathogenic *Escherichia coli*, *J Bacteriol* **188**: 2801-2811.

Oppenheim, A.B., Kobiler, O., Stavans, J., Court, D.L., and Adhya, S. (2005) Switches in bacteriophage lambda development, *Annu Rev Genet* **39**: 409-429.

Ozdemir, T., Fedorec, A.J.H., Danino, T., and Barnes, C.P. (2018) Synthetic Biology and Engineered Live Biotherapeutics: Toward Increasing System Complexity, *Cell Syst* **7**: 5-16.

Piñero-Lambea, C., Bodelón, G., Fernández-Periañez, R., Cuesta, A.M., Álvarez-Vallina, L., and Fernández, L.Á. (2015) Programming controlled adhesion of *E. coli* to target surfaces, cells, and tumors with synthetic adhesins, *ACS synthetic biology* **4**: 463-473.

Piñero-Lambea, C., Ruano-Gallego, D., and Fernández, L.A. (2015) Engineered bacteria as therapeutic agents, *Curr Opin Biotechnol* **35**: 94-102.

Politi, N., Pasotti, L., Zucca, S., Casanova, M., Micoli, G., Cusella De Angelis, M.G., and Magni, P. (2014) Half-life measurements of chemical inducers for recombinant gene expression, *Journal of biological engineering* **8**: 5.

Portaliou, A.G., Tsolis, K.C., Loos, M.S., Zorzini, V., and Economou, A. (2016) Type III Secretion: Building and Operating a Remarkable Nanomachine, *Trends Biochem Sci* **41**: 175-189.

Posfai, G., Kolisnychenko, V., Bereczki, Z., and Blattner, F.R. (1999) Markerless gene replacement in *Escherichia coli* stimulated by a double-strand break in the chromosome, *Nucleic Acids Res* **27**: 4409-4415.

Posfai, G., Plunkett, G., 3rd, Feher, T., Frisch, D., Keil, G.M., Umenhoffer, K., et al. (2006) Emergent properties of reduced-genome *Escherichia coli*, *Science* **312**: 1044-1046.

Quinn, J.Y., Cox, R.S., 3rd, Adler, A., Beal, J., Bhatia, S., Cai, Y., et al. (2015) SBOL Visual: A Graphical Language for Genetic Designs, *PLoS Biol* **13**: e1002310.

Riglar, D.T., and Silver, P.A. (2018) Engineering bacteria for diagnostic and therapeutic applications, *Nat Rev Microbiol* **16**: 214-225.

Rosano, G.L., and Ceccarelli, E.A. (2014) Recombinant protein expression in *Escherichia coli*: advances and challenges, *Front Microbiol* **5**: 172.

Roux, A., Beloin, C., and Ghigo, J.M. (2005) Combined inactivation and expression strategy to study gene function under physiological conditions: application to identification of new *Escherichia coli* adhesins, *J Bacteriol* **187**: 1001-1013.

Ruano-Gallego, D., Alvarez, B., and Fernandez, L.A. (2015) Engineering the Controlled Assembly of Filamentous Injectisomes in *E. coli* K-12 for Protein Translocation into Mammalian Cells, *ACS synthetic biology* **4**: 1030-1041.

Sauer, R.T., Ross, M.J., and Ptashne, M. (1982) Cleavage of the lambda and P22 repressors by recA protein, *J Biol Chem* **257**: 4458-4462.

Schuller, A., Cserjan-Puschmann, M., Tauer, C., Jarmer, J., Wagenknecht, M., Reinisch, D., et al. (2020) *Escherichia coli* σ70 promoters allow expression rate control at the cellular level in genome-integrated expression systems, *Microbial Cell Factories* **19**: 58.

Sekiya, K., Ohishi, M., Ogino, T., Tamano, K., Sasakawa, C., and Abe, A. (2001) Supermolecular structure of the enteropathogenic *Escherichia coli* type III secretion system and its direct interaction with the EspA-sheath-like structure, *Proc Natl Acad Sci U S A* **98**: 11638-11643.

Stalker, D.M., Kolter, R., and Helinski, D.R. (1982) Plasmid R6K DNA replication. I. Complete nucleotide sequence of an autonomously replicating segment, *J Mol Biol* **161**: 33-43.

Vo, J.L., Martinez Ortiz, G.C., Subedi, P., Keerthikumar, S., Mathivanan, S., Paxman, J.J., and Heras, B. (2017) Autotransporter Adhesins in *Escherichia coli* Pathogenesis, *Proteomics* **17**.

738 Voigt, C.A. (2006) Genetic parts to program bacteria, *Curr Opin Biotechnol* **17**: 548-
739 557.

740 Walker, B.J., Stan, G.V., and Polizzi, K.M. (2017) Intracellular delivery of biologic
741 therapeutics by bacterial secretion systems, *Expert reviews in molecular medicine* **19**:
742 e6.

743 Wilson, C.J., Zhan, H., Swint-Kruse, L., and Matthews, K.S. (2007) The lactose
744 repressor system: paradigms for regulation, allosteric behavior and protein folding, *Cell*
745 *Mol Life Sci* **64**: 3-16.

746 Wyborski, D.L., and Short, J.M. (1991) Analysis of inducers of the E.coli lac repressor
747 system in mammalian cells and whole animals, *Nucleic Acids Res* **19**: 4647-4653.

748 Zheng, W., Pena, A., Ilangovan, A., Baghshomali, Y.N., Frankel, G., Egelman, E.H.,
749 and Costa, T.R.D. (2021) Cryoelectron-microscopy structure of the enteropathogenic
750 *Escherichia coli* type III secretion system EspA filament, *Proc Natl Acad Sci U S A* **118**.
751
752

753
754 **Table 1. Bacterial strains used in this work.**

Name	Relevant genotype	Reference
BW25141	(F- l-) Δ*(araD-araB)567*, Δ*lacZ4787*(::rrnB-3), Δ*(phoB-phoR)580*, *galU95*, Δ*uidA3*::*pir*, *recA1*, *endA9*(del-ins)*::FRT*, *rph-1*, Δ*(rhaD-rhaB)568*, *hsdR51*	(Datsenko and Wanner, 2000)
SIEC	EcM1-Δ*yeeJ*::*Ptac*-eLEE2 Δ*yra*::*Ptac*-eLEE3 Δ*yfc*::*Ptac*-eEscD Δ*yebT*::*Ptac*-eLEE4 Δ*yfaL*::*Ptac*-eLEE1	(Ruano-Gallego, et al., 2015)
SIECΔ*lacI*	SIEC Δ*lacI*	This work
SIEC-I	SIEC Δ*lacI csg*::3R-I (*tetR-Ptet-cI*$^{+}$*Ind*$^{-}$, P_R-*lacI*^{W220F})	This work
SIEC-L	SIEC Δ*lacI csg*::3R-L (*tetR-Ptet-cI*$^{+}$*Ind*$^{-}$, P_R-*lacI*$^{W220F\text{-}LAA}$)	This work
SIEC-A	SIEC Δ*lacI csg*::3R-A (*tetR-Ptet-cI*$^{+}$*Ind*$^{-}$, P_R-*lacI*$^{W220F\text{-}AAV}$)	This work
SIEC-X	SIEC ΔlacI *csg*::3R-X (*tetR-Ptet-cI*$^{+}$*Ind*$^{-}$, P_R-*lacI*$^{W220F\text{-}ASV}$)	This work
SIEC-X2	SIEC Δ*lacI csg*::3R-X2 (*tetR-Ptet-cI*$^{+}$*Ind*$^{-}$, P_R-RBS0034-*lacI*$^{W220F\text{-}ASV}$)	This work
SIEC-X3	SIEC Δ*lacI csg*::3R-X3 (*tetR-Ptet-cI*$^{+}$*Ind*$^{-}$, P_R-RBS0034-$_{GTG}$*lacI*$^{W220F\text{-}ASV}$)	This work
SIEC-XLon	SIEC Δ*lacI csg*::3R-XLon (*tetR-Ptet-cI*$^{+}$*Ind*$^{-}$ *mf-Lon*, P_R-*lacI*$^{W220F\text{-}mf\text{-}ssrA\ tag}$)	This work
SIEC-GFP	SIEC *ypjA*::*Ptac*-GFP	This work
SIEC-I-GFP	SIEC Δ*lacI csg*::3R-I *ypjA*::*Ptac*-GFP	This work
SIEC-X-GFP	SIEC ΔlacI *csg*::3R-X *ypjA*::*Ptac*-GFP	This work
SIEC-XLon-GFP	SIEC Δ*lacI csg*::3R-XLon *ypjA*::*Ptac*-GFP	This work

755
756
757
758

Table 2. Plasmids used in this work.

Name	Features	Reference / Genebank
pGE	Km^R; R6K *ori*, I-SceI restriction sites flanking multicloning site.	(Piñero-Lambea, et al., 2015)
pACBSR-Sp	Sp^R, p15A ori, *araC*, P_{BAD}, *I-SceI* and λ Red genes	(Ruano-Gallego, et al., 2015)
pGEΔ*lacI*	pGE; HRs for deletion of *lacI-lacZ* in *E. coli* K-12	This work
pECL275	Plasmid template for amplification of *mf-lon*	(Cameron and Collins, 2014)
pGE*csg*3R-I	pGE; for integration of 3R-I in *csg* locus	This work / OR062285
pGE*csg*3R-L	pGE; for integration of 3R-L in *csg* locus	This work / OR062286
pGE*csg*3R-A	pGE; for integration of 3R-A in *csg* locus	This work / OR062284
pGE*csg*3R-X	pGE; for integration of 3R-X in *csg* locus	This work / OR062287
pGE*csg*3R-X2	pGE; for integration of 3R-X2 in *csg* locus	This work / OR062288
pGE*csg*3R-X3	pGE; for integration of 3R-X3 in *csg* locus	This work / OR062289
pGE*csg*3R-XLon	pGE; for integration of 3R-XLon in *csg* locus	This work / OR062290
pGE*ypjAPtac*-GFP	pGE; for integration of *Ptac-gfp*^{TCD} in *ypjA* locus	This work

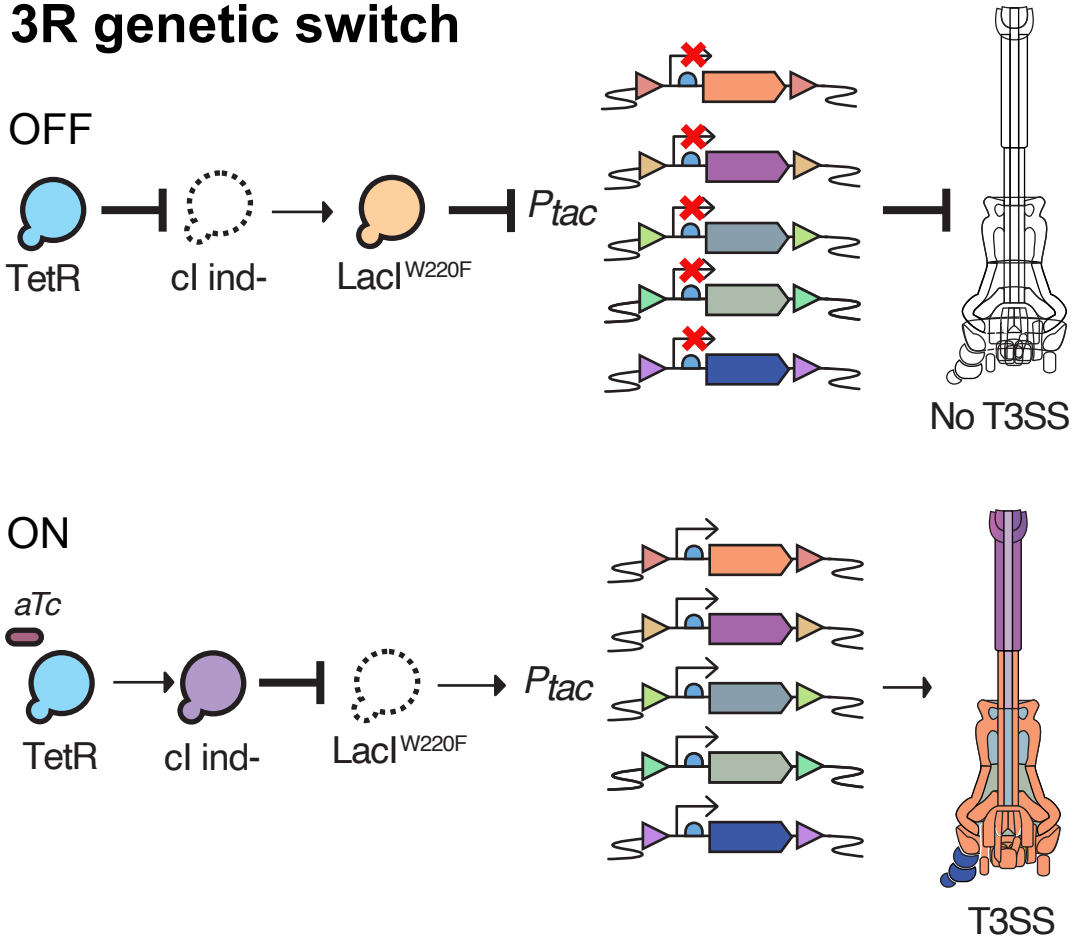

Graphical Abstract

Figure Legends

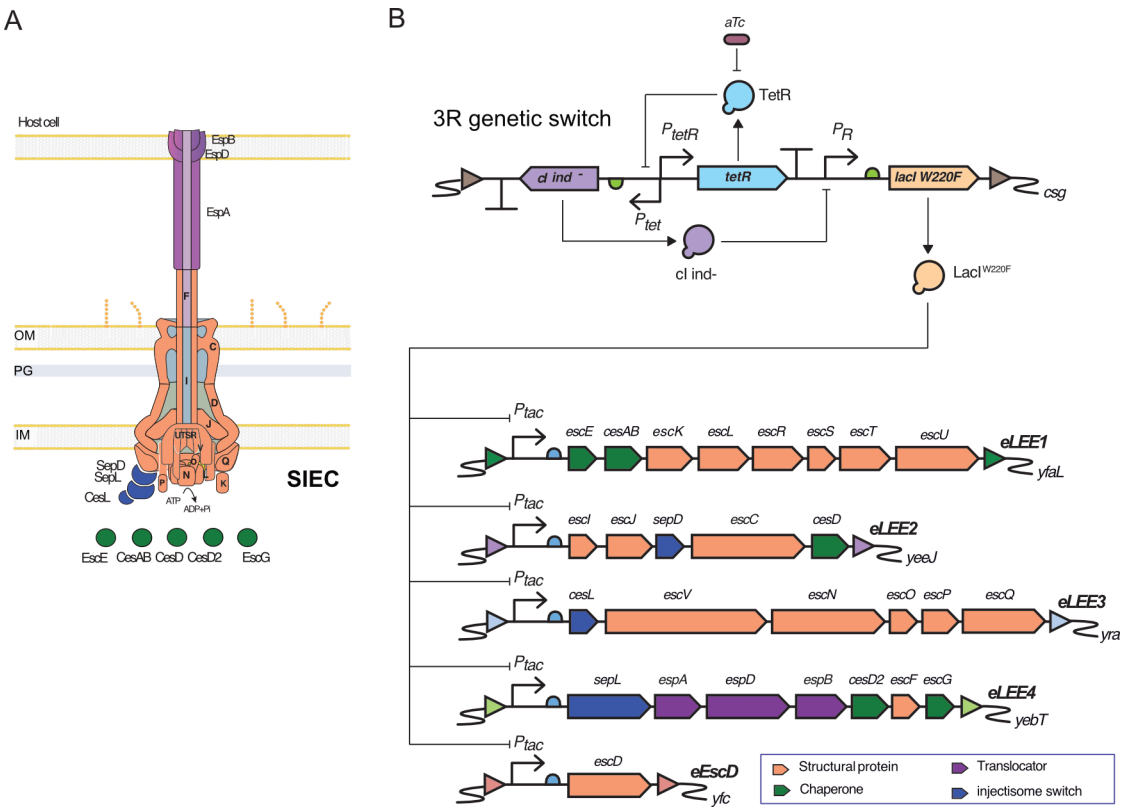

Figure 1. The three repressors (3R) genetic switch to control *Ptac* expression in the Synthetic Injector *E. coli* (SIEC) strain. (**A**) Scheme of the type III secretion system (T3SS) injectisome assembled by SIEC in the cell envelope (inner membrane, IM; peptidoglycan, PG; outer membrane, OM) to translocate proteins from the cytoplasm of bacteria to the host cell. (**B**) Diagram of the 3R switch for anhydrotetracycline (aTc) inducible control of P*tac* promoters in the synthetic eLEE operons encoding the T3SS components of the injectisome. Diagram representing parts (TetR, cI ind-, $LacI^{W220F}$) and interactions of the regulation circuit (upper part) and the T3SS operons of SIEC strain (lower part). Integration sites of the different constructs are indicated on the right (*csg*, *yfaL*, *yeeJ*, *yra*, *yeb*T, and *yfc*). See text for details. Visual glyphs following the Synthetic Biology Open Language standards (SBOL Visual) (Galdzicki, et al., 2014).

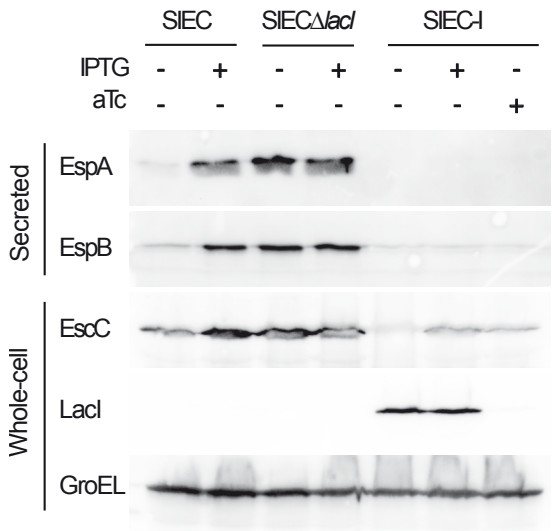

Figure 2. **Lack of T3SS induction by the 3R-I switch**. western blots to determine expression of T3SS components (EspA, EspB, EscC) and LacI/LacI^{W220F} in the bacterial strains SIEC, SIEC∆*lacI*, and SIEC-I (with 3R-I switch), grown and induced with IPTG or aTc as indicated (+, -). Western blots developed with specific antibodies to detect secreted EspA and EspB in the culture supernatants and LacI/LacI^{W220F} and EscC in whole-cell protein extracts. Detection of cytoplasmic GroEL is shown as loading control of the whole-cell protein extracts.

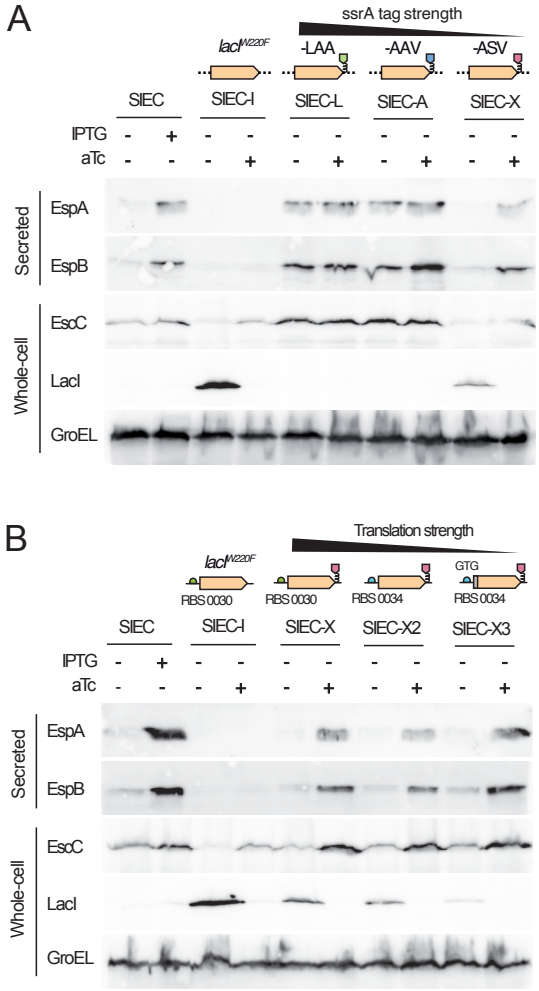

Figure 3. Function of 3R switches with LacI^{W220F} variants having different ssrA degradation tags and RBS. Western blots to determine expression of T3SS components (EspA, EspB, EscC) and LacI/LacI^{W220F} in the indicated bacterial strains carrying: (**A**) endogenous LacI (SIEC), the 3R-I switch with LacI^{W220F} (SIEC-I), the 3R switches with LacI^{W220F} fused to ssrA degradation tags LAA (SIEC-L), AAV (SIEC-A), and ASV (SIEC-X); (**B**) endogenous LacI (SIEC), the 3R-I switch with LacI^{W220F} (SIEC-I), the 3R switches with LacI^{W220F} fused to ssrA degradation tag ASV and RBS 0030 (SIEC-X), or RBS 0034 (SIEC-X2), or RBS 0034 in combination with GTG start codon (SIEC-X3). Bacteria were induced with IPTG or aTc as indicated (+, -). Western blots developed as in Fig. 2.

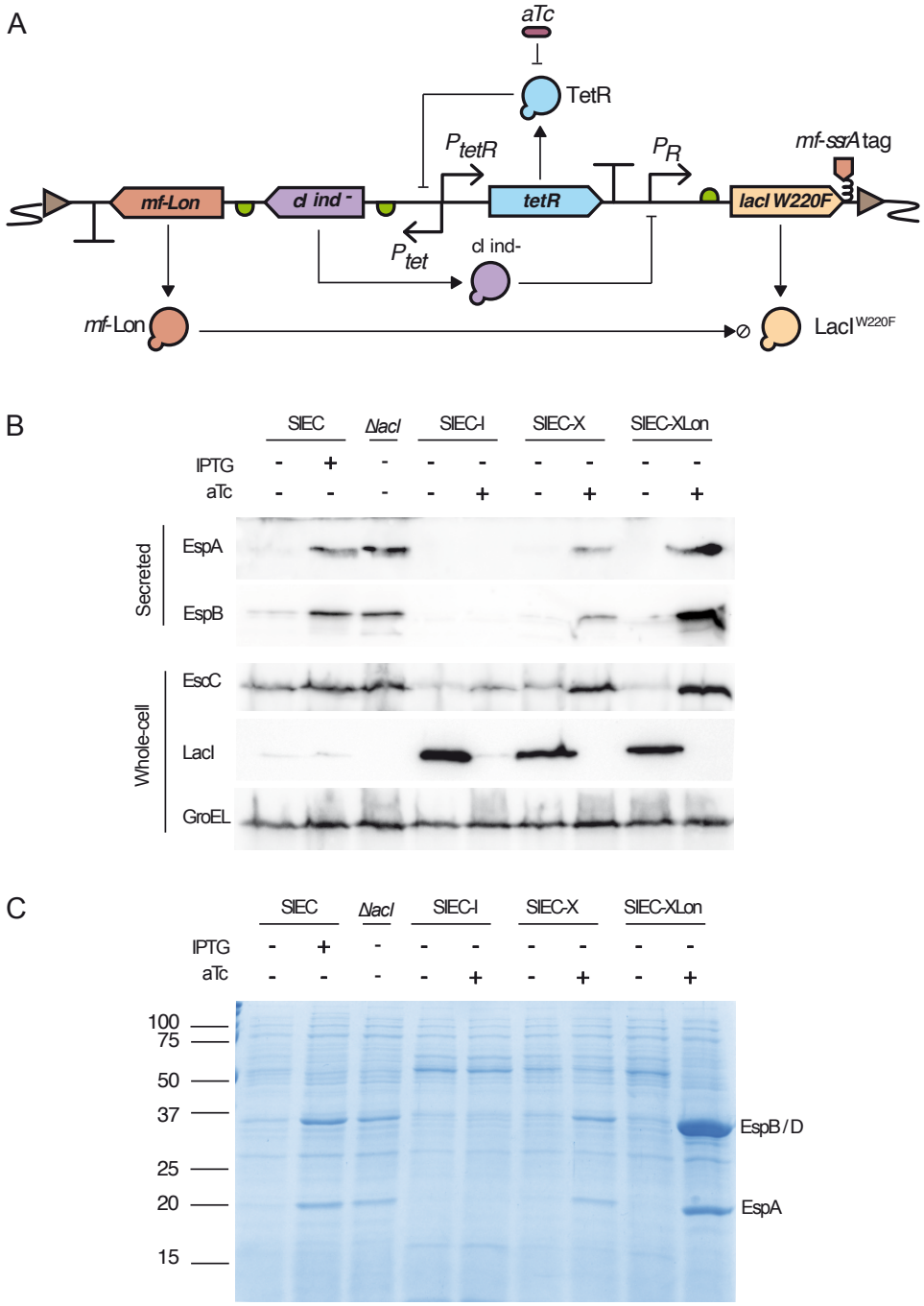

Figure 4. Function of 3R-XLon switch with orthogonal protein degradation system. (**A**) Diagram of the 3R-XLon regulatory circuit with the inducible *mf*-Lon protease (in the ON state) to degrade LacI^{W220F} with *mf*-ssrA tag. Visual glyphs following the Synthetic Biology Open Language standards (SBOL Visual). (**B**) Western blots to determine expression of T3SS components (EspA, EspB, EscC) and LacI/LacI^{W220F} in the indicated bacterial strains: SIEC, SIECD*lacI*, SIEC-I, SIEC-X and SIEC-XLon, having the 3R-XLon switch, induced with IPTG or aTc as indicated (+, -). Western blots developed as in Fig. 2. (**C**) Coomassie stained SDS-PAGE of proteins concentrated from supernatants of the induced cultures in B. The protein bands of secreted EspA, EspB (and EspD) are labeled. EspD migrates with EspB under the experimental conditions used. Mass of protein standards are shown on the left (in kDa).

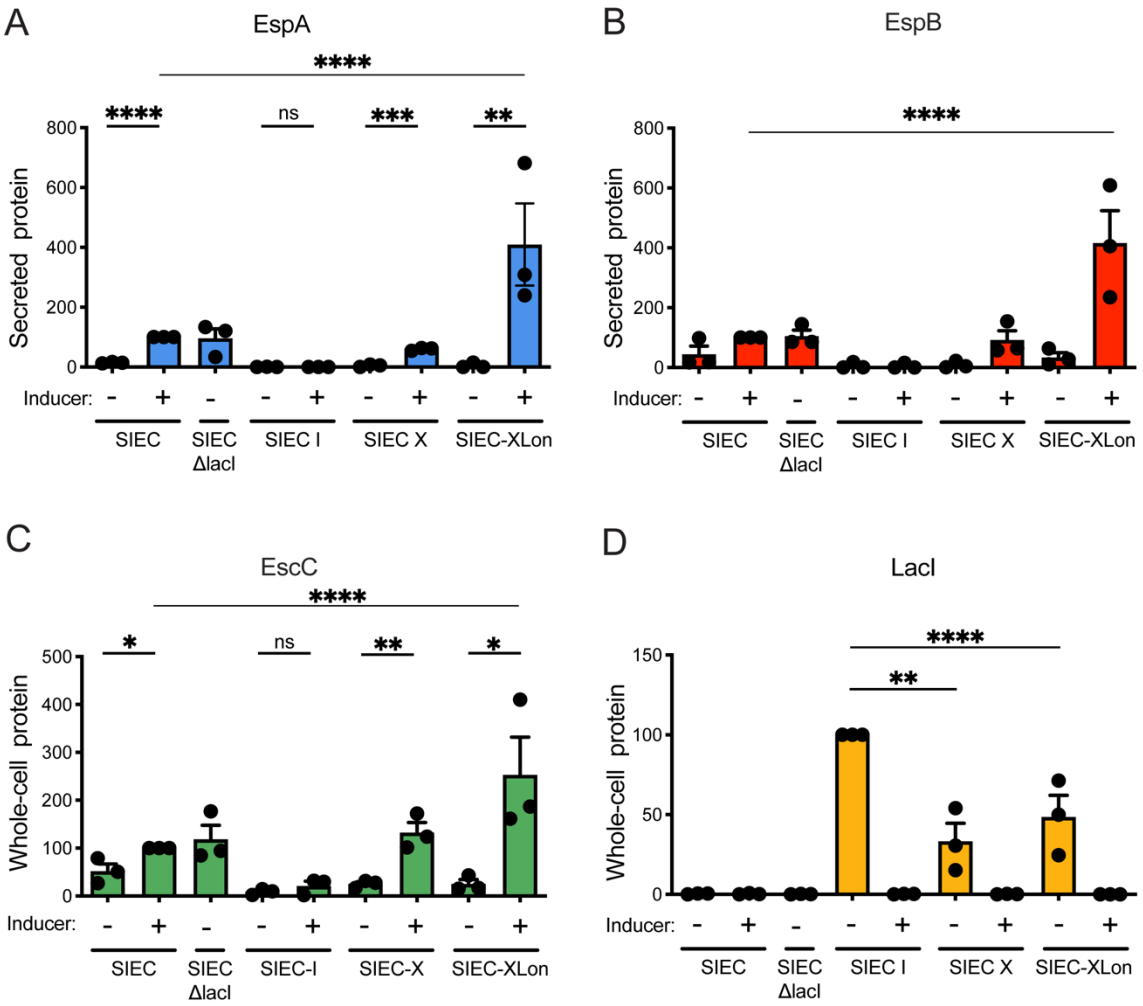

Figure 5. Quantification of T3SS proteins and LacI repressor in SIEC strains with 3R switches. The graphs show the normalized levels of secreted EspA (**A**), EspB (**B**), and in cell-associated EscC (**C**) and LacI (**D**), of the indicated SIEC strains induced with IPTG (for SIEC) or aTc as shown (+, -). Western blot signals (luminescence arbitrary units) of the corresponding protein bands were quantified and normalized relative to induced SIEC (in A, B and C) or relative to non-induced SIEC-I (in D), in both cases referred as 100. Growth an induction conditions as in Figure 2. Data from three independent experiments (n=3). Statistical significance inferred by unpaired t-test analysis, (*) p-value<0.05, (**) p-value<0.01, (***) p-value<0.001, (****) p-value<0.0001.

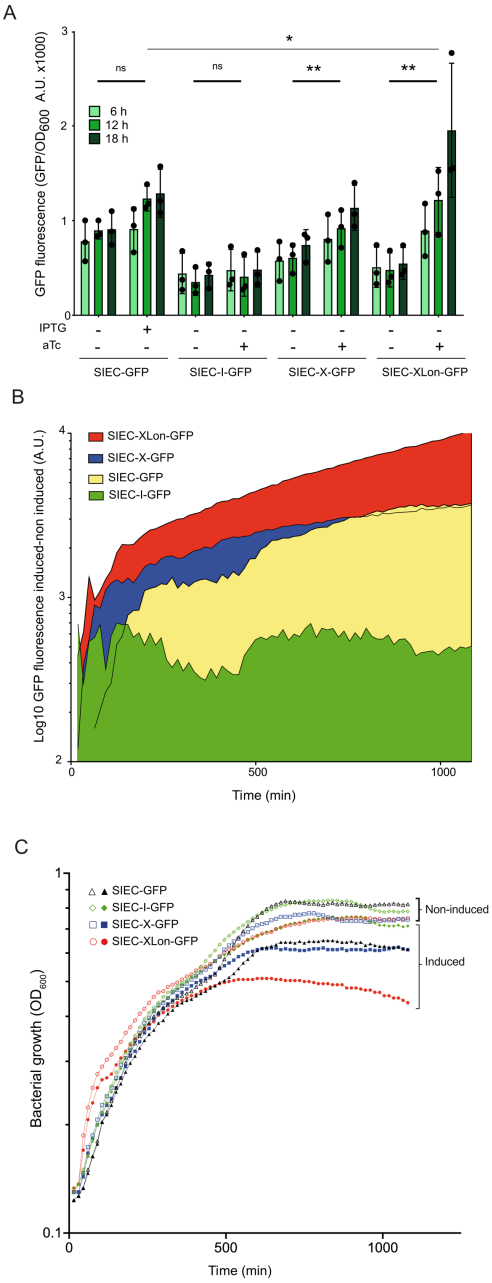

Figure 6. Performance of 3R switches quantified with a GFP reporter. (**A**) GFP expression under the control of a *tac* promoter (*Ptac-gfp*) integrated the chromosome and regulated by the endogenous LacI (SIEC) and different versions of the 3R switch in SIEC-I, SIEC-X and SIEC-XLon strains. Bars represent mean of GFP fluorescence normalized per OD_{600} at 6, 12 and 18 h post induction with appropriate inductor molecule, IPTG or aTc as indicated (+, -) from three independent experiments each including 6 technical replicas. Light green, medium green and dark green bars correspond to 6, 12 or 18 hours of induction respectively. Statistical significance inferred by two-way repeated measures (RM) ANOVA, (*) p-value<0.05, (**) p-value<0.01. (**B**) Dynamic range time evolution for GFP production in the same strains as in A. Graph represents mean of dynamic range of GFP fluorescence normalized per OD_{600} measured every 15 minutes, from three independent experiments each including 6 technical replicas. (**C**) Growth curves of the strains used in A, induced (filled symbols) and non-induced (open symbols) as indicated. Graph represents mean of OD_{600} values for each strain and growth conditions measured every 15 minutes, from three independent experiments each including 6 technical replicas.